



UNIVERSITY OF LEEDS

This is a repository copy of *Hypomorphic CARD11 mutations associated with diverse immunologic phenotypes with or without atopic disease.*

White Rose Research Online URL for this paper:
<http://eprints.whiterose.ac.uk/135712/>

Version: Accepted Version

Article:

Dorjbal, B, Stinson, JR, Ma, CA et al. (52 more authors) (2019) Hypomorphic CARD11 mutations associated with diverse immunologic phenotypes with or without atopic disease. *The Journal of Allergy and Clinical Immunology*, 143 (4). pp. 1482-1495. ISSN 0091-6749

<https://doi.org/10.1016/j.jaci.2018.08.013>

Published by Elsevier Inc. on behalf of the American Academy of Allergy, Asthma & Immunology. Licensed under the Creative Commons Attribution-NonCommercial-NoDerivatives 4.0 International
<http://creativecommons.org/licenses/by-nc-nd/4.0/>

Reuse

This article is distributed under the terms of the Creative Commons Attribution-NonCommercial-NoDeriv (CC BY-NC-ND) licence. This licence only allows you to download this work and share it with others as long as you credit the authors, but you can't change the article in any way or use it commercially. More information and the full terms of the licence here: <https://creativecommons.org/licenses/>

Takedown

If you consider content in White Rose Research Online to be in breach of UK law, please notify us by emailing eprints@whiterose.ac.uk including the URL of the record and the reason for the withdrawal request.



eprints@whiterose.ac.uk
<https://eprints.whiterose.ac.uk/>

Accepted Manuscript

Hypomorphic *CARD11* mutations associated with diverse immunologic phenotypes with or without atopic disease

Batsukh Dorjbal, PhD, Jeffrey R. Stinson, PhD, Chi A. Ma, PhD, Michael A. Weinreich, MD, Bahar Miraghazadeh, PhD, Julia M. Hartberger, Stefanie Frey-Jakobs, PhD, Stephan Weidinger, MD, Lena Moebus, MSc, Andre Franke, PhD, Alejandro A. Schäffer, PhD, Alla Bulashevskaya, PhD, Sebastian Fuchs, PhD, Stephan Ehl, MD, PhD, Sandhya Limaye, PhD, Peter D. Arkwright, FRCPCH, DPhil, Tracy A. Briggs, MBChB, PhD, Claire Langley, PhD, Claire Bethune, MRCP, MRCPATH, Andrew F. Whyte, MBBS, Hana Alachkar, MD, Sergey Nejentsev, MD, PhD, Thomas DiMaggio, RN, Celeste G. Nelson, CRNP, Kelly D. Stone, MD, Martha Nason, PhD, Erica H. Brittain, PhD, Andrew J. Oler, PhD, Daniel P. Veltri, PhD, T. Ronan Leahy, PhD, Niall Conlon, FRCPATH, PhD, Maria C. Poli, MD, Arturo Borzutzky, MD, Jeffrey I. Cohen, MD, Joie Davis, APRN, APRG, Michele P. Lambert, MD, Neil Romberg, MD, Kathleen E. Sullivan, MD, PhD, Kenneth Paris, MD, PhD, Alexandra F. Freeman, M.D., Laura Lucas, RN, Shanmuganathan Chandrasakan, MD, Sinisa Savic, MRCP, FRCPATH, Sophie Hambleton, MD, PhD, Smita Y. Patel, MD, PhD, FRCPATH, Michael B. Jordan, MD, Amy Theos, MD, Jeffrey Lebensburger, MD, T. Prescott Atkinson, MD, Troy R. Torgerson, MD, PhD, Ivan K. Chinn, MD, Joshua D. Milner, MD, Bodo Grimbacher, MD, Matthew C. Cook, MBBS, PhD, Andrew L. Snow, PhD

PII: S0091-6749(18)31201-6

DOI: [10.1016/j.jaci.2018.08.013](https://doi.org/10.1016/j.jaci.2018.08.013)

Reference: YMAI 13580

To appear in: *Journal of Allergy and Clinical Immunology*

Received Date: 23 April 2018

Revised Date: 2 August 2018

Accepted Date: 13 August 2018

Please cite this article as: Dorjbal B, Stinson JR, Ma CA, Weinreich MA, Miraghazadeh B, Hartberger JM, Frey-Jakobs S, Weidinger S, Moebus L, Franke A, Schäffer AA, Bulashevskaya A, Fuchs S, Ehl S, Limaye S, Arkwright PD, Briggs TA, Langley C, Bethune C, Whyte AF, Alachkar H, Nejentsev S, DiMaggio T, Nelson CG, Stone KD, Nason M, Brittain EH, Oler AJ, Veltri DP, Leahy TR, Conlon N, Poli MC, Borzutzky A, Cohen JI, Davis J, Lambert MP, Romberg N, Sullivan KE, Paris K, Freeman

AF, Lucas L, Chandrasakan S, Savic S, Hambleton S, Patel SY, Jordan MB, Theos A, Lebensburger J, Atkinson TP, Torgerson TR, Chinn IK, Milner JD, Grimbacher B, Cook MC, Snow AL, Hypomorphic *CARD11* mutations associated with diverse immunologic phenotypes with or without atopic disease, *Journal of Allergy and Clinical Immunology* (2018), doi: 10.1016/j.jaci.2018.08.013.

This is a PDF file of an unedited manuscript that has been accepted for publication. As a service to our customers we are providing this early version of the manuscript. The manuscript will undergo copyediting, typesetting, and review of the resulting proof before it is published in its final form. Please note that during the production process errors may be discovered which could affect the content, and all legal disclaimers that apply to the journal pertain.

1 **Hypomorphic *CARD11* mutations associated with diverse immunologic**
 2 **phenotypes with or without atopic disease.**

3
 4 Batsukh Dorjbal, PhD^a, Jeffrey R. Stinson, PhD^a, Chi A. Ma, PhD^b, Michael A.
 5 Weinreich, MD^b, Bahar Miraghazadeh, PhD^{c,d}, Julia M. Hartberger^e, Stefanie Frey-
 6 Jakobs, PhD^e, Stephan Weidinger, MD^f, Lena Moebus, MSc^f, Andre Franke, PhD^g,
 7 Alejandro A. Schäffer, PhD^h, Alla Bulashevskaya, PhD^e, Sebastian Fuchs, PhD^e, Stephan
 8 Ehl, MD, PhD^e, Sandhya Limaye, PhDⁱ, Peter D. Arkwright, FRCPCH, DPhil^j, Tracy A.
 9 Briggs, MBChB, PhD^j, Claire Langley, PhD^j, Claire Bethune, MRCP, MRCPATH^k, Andrew
 10 F. Whyte, MBBS^k, Hana Alachkar, MD^l, Sergey Nejentsev, MD, PhD^m, Thomas
 11 DiMaggio, RN^b, Celeste G. Nelson, CRNP^b, Kelly D. Stone, MD^b, Martha Nason, PhDⁿ,
 12 Erica H. Brittain, PhDⁿ, Andrew J. Oler, PhD^o, Daniel P. Veltri, PhD^o, T. Ronan Leahy,
 13 PhD^p, Niall Conlon, FRCPATH, PhD^q, Maria C. Poli, MD^r, Arturo Borzutzky, MD^s, Jeffrey
 14 I. Cohen, MD^t, Joie Davis, APRN, APRG^u, Michele P. Lambert, MD^v, Neil Romberg,
 15 MD^v, Kathleen E. Sullivan, MD, PhD^v, Kenneth Paris, MD, PhD^w, Alexandra F.
 16 Freeman^u, M.D., Laura Lucas, RN^x, Shanmuganathan Chandrasakan, MD^x, Sinisa
 17 Savic, MRCP, FRCPATH^y, Sophie Hambleton, MD, PhD^z, Smita Y Patel, MD, PhD,
 18 FRCPATH^{aa}, Michael B. Jordan, MD^{bb}, Amy Theos, MD^{cc}, Jeffrey Lebensburger, MD^{dd}, T.
 19 Prescott Atkinson, MD^{ee}, Troy R. Torgerson, MD, PhD^{ff}, Ivan K. Chinn, MD^r, Joshua D.
 20 Milner, MD^{bx}, Bodo Grimbacher, MD^{ex}, Matthew C. Cook, MBBS, PhD^{c,d*}, Andrew L.
 21 Snow, PhD^{a*}

22
 23 ^a Department of Pharmacology & Molecular Therapeutics, Uniformed Services
 24 University of the Health Sciences, Bethesda, MD, USA

25
 26 ^b Laboratory of Allergic Diseases, National Institute of Allergy and Infectious Diseases,
 27 National Institutes of Health, Bethesda, MD, USA

28
 29 ^c Department of Immunology, Canberra Hospital, ACT Australia

30
 31 ^d Centre for Personalised Immunology, John Curtin School of Medical Research,
 32 Australian National University, Canberra, Australia

33
 34 ^e Center for Chronic Immunodeficiency (CCI), Medical Center – University of Freiburg,
 35 Faculty of Medicine, University of Freiburg, Germany

36
 37 ^f Department of Dermatology, Venereology and Allergology, University Hospital
 38 Schleswig-Holstein, Campus Kiel, Kiel, Germany

39
 40 ^g Institute of Clinical Molecular Biology, Christian-Albrechts-University of Kiel, Germany

41
 42 ^h National Center for Biotechnology Information, National Institutes of Health,
 43 Department of Health and Human Services, Bethesda, MD, USA

44
 45 ⁱ Repatriation and General Hospital, Concord, Australia

46

- 47 ^j Paediatric Allergy and Immunology & Manchester Center for Genomic Medicine,
48 University of Manchester, Manchester, Manchester, UK
49
- 50 ^k Department of Clinical Immunology, Plymouth Hospitals NHS Trust, Plymouth, UK
51
- 52 ^l Immunology, Salford Royal Foundation Trust, Manchester, UK
53
- 54 ^m Department of Medicine, University of Cambridge, Cambridge, UK
55
- 56 ⁿ Biostatistics Research Branch, National Institute of Allergy and Infectious Diseases,
57 National Institutes of Health, Bethesda, MD, USA
58
- 59 ^o Bioinformatics and Computational Sciences Branch, Office of Cyber Infrastructure and
60 Computational Biology, National Institute of Allergy and Infectious Diseases, National
61 Institutes of Health, Bethesda, MD, USA
62
- 63 ^p Department of Paediatric Immunology and ID, Our Lady's Children's Hospital, Crumlin,
64 Dublin, Ireland
65
- 66 ^q Department of Immunology, St James's Hospital, Dublin, Ireland
67
- 68 ^r Department of Pediatrics, Baylor College of Medicine, Houston, TX, USA
69 Section of Immunology, Allergy, and Rheumatology, Texas Children's Hospital,
70 Houston, TX, USA
71
- 72 ^s Department of Pediatrics, School of Medicine, Pontifical Catholic University of Chile,
73 Santiago, Chile
74
- 75 ^t Laboratory of Infectious Diseases, National Institute of Allergy and Infectious Diseases,
76 US National Institutes of Health, Bethesda, MD, USA.
77
- 78 ^u Laboratory of Clinical Immunology and Microbiology, National Institute of Allergy and
79 Infectious Diseases, US National Institutes of Health, Bethesda, MD, USA.
80
- 81 ^v Division of Immunology and Allergy, The Children's Hospital of Philadelphia,
82 Philadelphia, PA, USA; Department of Pediatrics, The Perelman School of Medicine at
83 the University of Pennsylvania, Philadelphia, PA, USA
84
- 85 ^w Louisiana State University Health Sciences Center and Children's Hospital, New
86 Orleans, LA, USA
87
- 88 ^x Division of Bone Marrow Transplant, Children's Healthcare of Atlanta,
89 Emory University School of Medicine, Atlanta, GA, USA
90
- 91 ^y Leeds Institute for Rheumatic and Musculoskeletal Medicine, St. James University
92 Hospital, Leeds, UK

93
94 ^z Primary Immunodeficiency Group, Institute of Cellular Medicine, Newcastle University,
95 Newcastle upon Tyne, UK

96
97 ^{aa} Oxford University Hospitals NHS Trust and NIHR Oxford Biomedical Research
98 Centre, Oxford, UK

99
100 ^{bb} Division of Bone Marrow Transplantation and Immune Deficiency, Department of
101 Pediatrics, Cincinnati Children's Hospital Medical Center, University of Cincinnati,
102 Cincinnati, OH, USA.

103
104 ^{cc} Department of Dermatology, University of Alabama at Birmingham, Birmingham, AL,
105 USA

106
107 ^{dd} Department of Pediatric Hematology Oncology, University of Alabama at Birmingham,
108 Birmingham, AL USA

109
110 ^{ee} Department of Pediatrics, University of Alabama at Birmingham, Birmingham, AL
111 USA

112
113 ^{ff} University of Washington School of Medicine and Seattle Children's Hospital, Seattle,
114 WA, USA.

115
116 *These authors contributed equally to the manuscript.

117
118
119 Corresponding author:

120
121 Dr. Andrew L. Snow
122 Department of Pharmacology & Molecular Therapeutics
123 Uniformed Services University of the Health Sciences
124 4301 Jones Bridge Road, C-2013
125 Bethesda, MD 20814 USA

126
127 Phone: (301) 295-3267
128 Email: andrew.snow@usuhs.edu

129

130 **Abstract**

131

132 **Background**

133 *CARD11* encodes a scaffold protein in lymphocytes that links antigen receptor
134 engagement with downstream signaling to NF- κ B, JNK, and mTORC1. Germline
135 *CARD11* mutations cause several distinct primary immune disorders in humans,
136 including SCID (biallelic null mutations), B cell Expansion with NF- κ B and T cell Anergy
137 (BENTA; heterozygous, gain-of-function mutations), and severe atopic disease (loss-of-
138 function, heterozygous, dominant interfering mutations), which has focused attention on
139 *CARD11* mutations discovered by whole exome sequencing.

140

141 **Objectives**

142 To determine the molecular actions of an extended allelic series of *CARD11*, and to
143 characterize the expanding range of clinical phenotypes associated with heterozygous
144 *CARD11* loss-of-function alleles.

145

146 **Methods**

147 Cell transfections and primary T cell assays were utilized to evaluate signaling and
148 function of *CARD11* variants.

149

150 **Results**

151 Here we report on an expanded cohort of patients harboring novel heterozygous
152 *CARD11* mutations that extend beyond atopy to include other immunologic phenotypes
153 not previously associated with *CARD11* mutations. In addition to (and sometimes
154 excluding) severe atopy, heterozygous missense and indel mutations in *CARD11*
155 presented with immunologic phenotypes similar to those observed in STAT3-LOF,
156 DOCK8 deficiency, common variable immune deficiency (CVID), neutropenia, and
157 immune dysregulation, polyendocrinopathy, enteropathy, X-linked (IPEX)-like
158 syndrome. Pathogenic variants exhibited dominant negative activity, and were largely
159 confined to the CARD or coiled-coil domains of the *CARD11* protein.

160

161 **Conclusion**

162 These results illuminate a broader phenotypic spectrum associated with *CARD11*
163 mutations in humans, and underscore the need for functional studies to demonstrate
164 that rare gene variants encountered in expected and unexpected phenotypes must
165 nonetheless be validated for pathogenic activity.

166

167

168 **Keywords:** *CARD11*; atopy; atopic dermatitis; dominant negative, primary
169 immunodeficiency, immune dysregulation

170

171 **Abbreviations:**

172 AHA: autoimmune hemolytic anemia

173 BENTA: B cell Expansion with NF- κ B and T cell Anergy

174 CARD: caspase activation and recruitment domain

175 CC: coiled-coil

176 CVID: common variable immunodeficiency

177 DN: dominant negative

178 EoE: eosinophilic esophagitis

179 EBV: Epstein-Barr virus

180 FTT: failure to thrive

181 GOF: gain-of-function

182 HSV-1: herpes simplex virus 1

183 IPEX: immune dysregulation, polyendocrinopathy, enteropathy, X-linked

184 ITP: idiopathic thrombocytopenic purpura

185 JNK: c-Jun N-terminal kinase

186 LGL: large granular lymphocytic leukemia

187 LOF: loss-of-function

188 MAGUK: membrane-associated guanylate kinase domain

189 MAS: macrophage activation syndrome

190 mTORC1: mechanistic target of rapamycin complex 1

191 PMA: Phorbol 12-myristate 13-acetate

192 NF- κ B: nuclear factor kappa B

193 SCID: severe combined immune deficiency

194 sJIA: systematic juvenile idiopathic arthritis

195 T1D/T2D: type 1 / type 2 diabetes

196 TCR: T cell receptor

197 WES: whole exome sequencing

198 WGS: whole genome sequencing

199

200 **Key Messages:**

201

- 202 • *CARD11* DN mutations are associated with a broader spectrum of human disease
203 phenotypes than previously appreciated, extending beyond atopy to include
204 cutaneous viral and respiratory infections, hypogammaglobulinemia, autoimmunity,
205 neutropenia, and lymphoma.
- 206
- 207 • Pathogenic DN mutations are most likely located in the N-terminal CARD and CC
208 domains of *CARD11*, compromising TCR-induced NF- κ B activation
- 209
- 210 • Clinicians should test for causative *CARD11* DN mutations in patients that present
211 with an autosomal dominant pattern of atopy, viral skin infections, and/or respiratory
212 infections and exhibit defective TCR-induced NF- κ B activation in vitro, with or
213 without impaired TCR-induced S6 phosphorylation.

214 **Capsule Summary**

215

216 This description of a large cohort of patients broadens the spectrum of clinical disease

217 phenotypes linked to *CARD11* DN mutations, including atopy, cutaneous viral and

218 respiratory infections, hypogammaglobulinemia, autoimmunity, neutropenia, and

219 lymphoma.

ACCEPTED MANUSCRIPT

220 **Introduction**

221

222 Hypomorphic mutations in genes whose protein products are critical for immune
223 function provide an opportunity to assess the protein's roles in the context of a
224 functioning, albeit impaired, immune response. Unlike the unresponsive or absent
225 effector compartments often associated with null mutations that manifest as severe
226 combined immune deficiency (SCID), these mutations preserve sufficient function to
227 allow for development of the particular cell(s) or organ(s) with which it is involved.
228 Studies of such allelic variants in mice and other model organisms have taught us much
229 about immune system development and function. With the wider availability and
230 application of next-generation sequencing technologies, we now have more
231 opportunities to explore the phenomenon of allelic variance and phenotypic
232 heterogeneity in humans. One example can be found in the case of *RAG1* – null
233 mutants lead to the absence of T-cells and grossly abnormal thymic development.
234 Hypomorphic mutations lead to functioning T-cells but disruptions of repertoire and
235 thymic development that shed light on immune tolerance, *RAG1* protein domain
236 function, and other immune processes (1).

237

238 Another example is found in different types of mutations described in *CARD11* leading
239 to different phenotypes. *CARD11* is a critical 1154 amino acid protein scaffold best
240 known for linking antigen recognition with downstream NF- κ B activation in lymphocytes
241 (2, 3). The protein *CARD11* (also known as *CARMA1*, represented by the sequences
242 NP_115791.3 and NM_032415) includes an N-terminal caspase recruitment domain
243 (CARD, 1-110), LATCH (112-130), coiled-coil (CC, 130-449) domains, and a C-terminal
244 membrane-associated guanylate kinase domain (MAGUK, 667-1140) comprised of
245 PDZ, SH3 and GUK domains. Biallelic null mutations of *CARD11*, in both patients and
246 mouse models, lead to severe T and B-cell immune deficiency (4). Somatic gain-of-
247 function (GOF) *CARD11* mutations are commonly found in non-Hodgkin B cell
248 lymphomas, whereas germline GOF mutations give rise to BENTA (B cell Expansion
249 with NF- κ B and T cell Anergy) disease in humans (2, 5, 6). Surprisingly,
250 hypomorphic/dominant negative (DN) mutations in both mice and human patients permit

251 sufficient effector function to reveal a strong disposition toward atopic phenotypes, in
252 addition to variable immune deficiency (7-9). Because *CARD11* oligomerization is
253 essential for downstream signaling, heterozygous variants can either enhance or
254 dominantly interfere with *CARD11* function (10, 11).

255
256 Greater access to next-generation sequencing virtually guarantees that variants in a
257 particular gene can now be identified in patients with ever-broadening phenotypes,
258 especially for cases of GOF and hypomorphic loss of function (LOF) mutations (12).
259 Although algorithms can assist in predicting which variants are likely to be benign or
260 deleterious, previously undescribed rare or novel variants in such genes must always be
261 validated for pathogenicity using relevant biological assays. Moreover, in silico
262 prediction methods do not distinguish between variants seen in the heterozygous state
263 and homozygous state, which is critical for *CARD11*. Furthermore, collection and testing
264 of variants from as many centers as possible can more accurately determine the
265 breadth of disease associated with a given gene, especially given the role that referral
266 bias can play in any given center.

267
268 We therefore report our experience with numerous heterozygous mutations in *CARD11*
269 in the context of severe familial atopic disease and other immunologic phenotypes not
270 previously associated with *CARD11* mutations. The atopy described here is a genetic
271 tendency to develop symptoms of immediate hypersensitivity (e.g. food allergy, allergic
272 rhinitis) or allergic inflammation (e.g. eczema, eosinophilic esophagitis), irrespective of
273 specific allergen sensitization (13). In many cases, rare or novel mutations were
274 uncovered in whole exome/genome sequences (WES/WGS) performed at major referral
275 centers for multiple reasons, particularly in patients without a clear putative genetic
276 diagnosis. Herein we attribute several new DN *CARD11* mutations to an expanded list
277 of disease manifestations, and describe assays designed to help differentiate
278 pathogenic vs. non-pathogenic variants in *CARD11*. Importantly, results of these assays
279 are interpreted within the context of specific genotypic/phenotypic criteria that help to
280 define a differential diagnosis for patients harboring *CARD11* DN mutations. In addition
281 to severe atopy, heterozygous missense mutations in *CARD11* with DN activity can

282 present with common variable immune deficiency (CVID), neutropenia, cutaneous viral
283 infections, and immunodysregulation polyendocrinopathy enteropathy X-linked (IPEX)-
284 like syndrome. Collectively, our findings define a broader spectrum of immune disease
285 associated with detrimental *CARD11* mutations, which are most often confined to
286 specific domains of the *CARD11* protein. Nevertheless, our evaluations underscore the
287 idea that rare gene variants found by WES/WGS can be pathogenic even when not
288 matching with reported phenotypes. At the same time, *CARD11* mutations associated
289 with an expected phenotype must nonetheless be validated for pathogenic activity using
290 functional studies.

291

292

293 **Methods**

294

295 *Patients*

296 Informed consent was obtained from all participating patients and their family members
297 according to protocols approved by Institutional Review Boards and ethics boards at
298 their respective institutions.

299

300 *Whole exome sequencing (WES) and genetic analysis*

301 WES was performed on the majority of patients described here according to established
302 protocols. For example, Kindreds 6, 19 and 29 were analyzed as follows. Genomic DNA
303 was extracted from peripheral blood cells and Illumina paired-end genomic DNA sample
304 preparation kit (PE-102-1001, Illumina) was used for preparing the libraries followed by
305 exome-enriched library using the Illumina TruSeq exome kit (FC-121-1008, Illumina).
306 Samples were sequenced on an Illumina HiSeq as 100-bp paired-end reads. DNA
307 reads were mapped to the GRCh38 human genome reference using the default
308 parameters of the Burrows-Wheeler Aligner (bio-bwa.sourceforge.net). Single
309 nucleotide substitutions and small insertion deletions were identified and filtered based
310 on quality with SAMtools software package (samtools.sourceforge.net) and annotated
311 with Annovar tool (www.openbioinformatics.org). Filtering of variants for novelty was
312 performed according to minor allele frequency, mouse mutant phenotype in the
313 homologous mouse gene, Mendelian disease associations (OMIM), pathway analysis
314 (gene ontology [GO]), immune system expression (Immgen), CADD, SIFT, and
315 PolyPhen-2 scores (14-16). After filtering and ranking variants, heterozygous *CARD11*
316 variants were investigated further.

317

318 Kindred 14 (R187P) was initially evaluated separately from the other families. Eight
319 samples were subjected to whole exome sequencing (WES) as described previously
320 (17) (Supplementary Materials and Methods). We selected putative causative variants
321 that had an average read depth ≥ 20 , a quality score of ≥ 200 , and were heterozygous in
322 at least one individual. Genetic analysis showed that seven of the samples were related
323 and one sample was not related. The remaining seven samples were from one

324 unaffected individual and six affected individuals. We did a combinatorial search for
325 variants present in the heterozygous state in the six affected individuals and absent in
326 the unaffected individual. We performed multipoint genetic linkage analysis with
327 Superlink-online-SNP (18, 19) assuming a rare disease allele and dominant inheritance.
328 Two variants satisfied the combinatorial condition of being heterozygous in six sampled
329 affected individuals and absent in the one sampled unaffected individual: MICALL2
330 (p.Q202*) and CARD11 (p.R187P), and were at the same time located in a region
331 (chr7:0.0-4.3 Mbp) consistent with genetic linkage.

332

333 *PBMC signaling analysis*

334 PBMC were isolated by Ficoll gradient centrifugation. Phosphorylation of p65 and/or S6,
335 and degradation of I κ B was assessed by intracellular flow cytometry after short ex vivo
336 stimulations with PMA as previously described (9). To assess S6 phosphorylation under
337 Th0 conditions, total PBMC (10^6 /ml) were seeded in 1 mL RPMI (Gibco) supplemented
338 with 10% FBS, penicillin/streptomycin and L-glutamine in an anti-CD3 antibody (OKT3,
339 1 μ g/mL) coated 48-well plate. Anti-CD28 antibody (L293, 0.2 μ g/mL,) and IL-2 (10
340 ng/mL, Peprotech) were then added to the culture (Th0), and cells were incubated in a
341 37°C CO₂ chamber. After 24 hours, cells were pelleted by centrifugation, stained with
342 Live/Dead dye (Thermo Fisher), fixed with 1.6% paraformaldehyde in PBS, then
343 centrifuged and permeabilized with absolute methanol. Cells were then stained for flow
344 cytometry with fluorochrome-conjugated antibodies after washes with FACS buffer (PBS
345 with 0.5% BSA). The antibodies (Abs) used for flow cytometry were: CD3 (UCHT1),
346 CD4 (RPA-T4, L200), CD45RA (HI100), phospho-S6 (N7-548) (BD Biosciences).
347 Percentages of phospho-S6⁺ live CD3⁺ CD4⁺ cells, gated on the lymphocyte SSC and
348 CD45RA compartments, are shown in Figure 6.

349

350 *CARD11 mutant expression plasmids*

351 Modified wild type (WT) and mutant pUNO-CARD11-FLAG plasmids were constructed
352 and purified as previously described (9). Briefly, site-directed mutagenesis was utilized
353 to introduce single nucleotide variants that were putative point mutations into the WT
354 CARD11 construct (Invivogen) using primer-directed linear amplification with Pwo or

355 PfuI polymerase (Roche), followed by *DpnI* digestion of methylated template DNA
356 (ThermoFisher). All inserted variants were confirmed by Sanger sequencing. All
357 resulting plasmids were purified from DH5 α E. Coli (New England Biolabs) using a
358 GenElute HP Plasmid Maxi-Prep Kit (Sigma).

359

360 *Cell transfection assays*

361 Both WT (clone E6.1, ATCC) and CARD11-deficient Jurkat T cells (referred to as
362 JPM50.6) were cultured and transfected as previously described (9). JPM50.6 cells
363 containing an integrated canonical NF- κ B-driven GFP reporter were originally provided
364 by Dr. Xin Lin (MD Anderson Cancer Center). Briefly, 5x10⁶ Jurkat or JPM50.6 T cells
365 were resuspended in 0.4 mL RPMI/10% FBS, placed in 0.4cm cuvettes (Bio-Rad) and
366 electroporated (260 V, 950 μ F) with 5-10 μ g plasmid DNA (BTX Harvard Apparatus).
367 For JPM50.6, cells were stimulated 24 hours post-transfection with 1 μ g/ml anti-
368 CD3/CD28 antibodies and incubated overnight (BD Biosciences). Relative canonical
369 NF- κ B activation in JPM50.6 was quantified based on mean fluorescence intensity
370 (MFI) of an integrated κ B-GFP reporter using an Accuri C6 flow cytometer (BD
371 Biosciences). To assess S6 phosphorylation in Jurkat transfectants, cells were washed
372 24 hrs post-transfection in PBS and incubated in PBS/1%BSA for 1 hr at 37°C.
373 Following an additional PBS wash, cells were stimulated with 1 μ g/ml anti-CD3/CD28
374 antibodies (BD Biosciences) for 20 min at 37°C. Activation was stopped by adding ice
375 cold PBS, and cells were pelleted and lysed in 1% NP-40 lysis buffer as previously
376 described (9). Lysates (5-10 μ g) were separated on 4-20% Tris-Glycine SDS gels and
377 transferred to nitrocellulose membranes (Bio-Rad). Membranes were blocked in 5%
378 milk/TBS/0.1%Tween20 and immunoblotted with the following Abs: anti-phospho-S6
379 (Ser235/236), anti-S6 (5G10), anti-CARD11 (1D12, Cell Signaling Technology; LS-
380 C368868, LifeSpan Biosciences; OASG00985, Aviva Systems Biology); anti-HA (2-
381 2.2.14, Thermo Fisher), anti-FLAG (M2) and anti- β -actin (AC-15, Sigma). Blots were
382 washed 3x in TBS/0.1%Tween20), incubated in HRP-conjugated secondary Abs
383 (Southern Biotech), and washed again. Bands were visualized by enhanced
384 chemiluminescence (Thermo Fisher) and imaged on a ChemiDoc system (Bio-Rad).

385 Spot densitometric quantification of phosphor-S6 vs. total S6 was performed using
386 ImageLab software (Bio-Rad).

387

388 *Hierarchical clustering analysis*

389 Hierarchical Clustering with a complete linkage algorithm and an asymmetric binary
390 distance measure (for binary variables) was used to explore the data contained in
391 Online Repository Table 1. Due primarily to a significant proportion of missing data
392 across many of the variables, only a subset of variables was included in the clustering
393 algorithm. Moreover, only subjects with complete data on the chosen subset were
394 included in the hierarchical clustering. Models were also run using different variable
395 sets, distance measures, and clustering algorithms, and led to different sets of
396 clusters. Hence presented results should be considered exploratory and descriptive.

397

398 *Unsupervised patient clustering*

399 To depict patients with their phenotypic attributes in 2-dimensional space, we used
400 Gower distance transformation (20) (as implemented in the daisy function in the R
401 cluster v2.0.7-1 package (21, 22), which handles datasets with missing data points,
402 followed by tSNE (23) as implemented in the Rtsne v0.13 library (using settings theta=0
403 and perplexity=10). Next, we divided the patient cohort into three clusters using K-
404 means clustering in R (K=3). The process of using tSNE and K-means to cluster
405 patients was repeated over 10 trials and consensus assignment was used to assign
406 each patient to a final cluster id. To identify phenotypes important for each cluster, we
407 performed attribute selection and logistic regression in Weka v3.8.2 (24). For attribute
408 selection, we used the Fast Correlation-based Feature Search method (25) to select
409 nonredundant attributes. Using the selected attributes, we performed multinomial
410 logistic regression using the SimpleLogistic function (26) with 5-fold cross-validation to
411 build a classifier for assigning patients to one of the three clusters. The features
412 selected along with their predicted coefficients allowed us to assess the importance of
413 phenotypes for each class separately. Based on 10 randomized trials, the classifier
414 demonstrated an overall accuracy of 88.1% with standard deviation (SD) $\pm 11.7\%$.

415 Sensitivity and specificity for the trials were 98.33% (SD: $\pm 8.42\%$) and 93.90% (SD:
416 $\pm 11.03\%$), respectively.

417

418 *Statistics*

419 For JPM50.6 transfections, two-way ANOVAs with Sidak correction were used to
420 compare GFP MFI between WT and mutant CARD11. pS6/total S6 protein
421 densitometric ratios were normalized to WT values and compared by a Wilcoxon
422 signed-rank test. For primary cell assays, experimental and technical replicates were
423 limited by small numbers of patient samples available. For patients in Kindreds 6, 19
424 and 29, ratios of pS6 gMFI (stimulated/unstimulated) were compared to healthy controls
425 (matched per experiment) using a Kruskal-Wallis test.

426 **Results**

427

428 **Novel dominant negative *CARD11* mutations detected in a broad spectrum of**
429 **immune disorders**

430 Rare or novel *CARD11* mutations were identified by allergy and primary
431 immunodeficiency referral centers in patients with immune-deficient or dysregulatory
432 phenotypes (Table 1). A total of 48 new patients in 27 families, with 26 different
433 heterozygous germline *CARD11* variants were referred. Salient patient phenotypes,
434 combined with those already reported (7, 9), are summarized in Tables 1-2. These
435 alleles were then evaluated at centers specialized in *CARD11* biology and associated
436 diseases and pathways. First, we investigated whether each variant altered T cell
437 receptor (TCR) signaling. Each *CARD11* variant was cloned into an expression
438 construct and transfected in WT Jurkat or *CARD11*-deficient Jurkat (JPM50.6) T cell
439 lines. As a control, we also tested a variant (p.C150L) identified as a somatic reversion
440 mutant that restored NF- κ B signaling in T cells from a *CARD11*-deficient patient that
441 developed Omenn's syndrome (27). Upon CD3/CD28 stimulation of transfected
442 JPM50.6 cells, 14/26 mutants demonstrated significantly reduced NF- κ B activation,
443 indicating loss of function (LOF) (Figure 1A). Two variants (p.P495S, p.R848C)
444 displayed enhanced NF- κ B activation only after stimulation; unlike BENTA-associated
445 mutations, these variants did not induce constitutive NF- κ B activity. As all variants were
446 heterozygous, we next tested whether each LOF mutant could dominantly interfere with
447 WT *CARD11* signaling when co-expressed at 50:50 ratios. Among 14 LOF mutations,
448 dominant negative (DN) activity (defined as significantly reduced NF- κ B activation
449 relative to 100% WT expression) was observed for 10 (Figure 1B). Most of these new
450 DN variants were confined to the CARD domain and proximal coiled-coil (CC) domains,
451 which are critical for both *CARD11* oligomerization and BCL10-MALT1 interactions (28,
452 29). All variants were comparably expressed in transfected cells, suggesting none of the
453 mutations tested affected *CARD11* protein translation and stability (Figure 1C and data
454 not shown). Although a faint 15 kD band was noted upon prolonged blot exposure, we
455 could not definitively confirm the presence of a truncated K143X protein by immunoblot
456 using available N-terminus specific *CARD11* Abs, which cross-reacted with many non-

457 specific proteins (data not shown). However, the fact that expression of this construct,
458 and not the Q945X truncation mutant (9), exhibits DN activity strongly suggests that it is
459 expressed. Moreover, a K143X CARD11 expression construct engineered to include a
460 C-terminal HA-tag was clearly expressed in JPM50.6 transfectants, and exhibited
461 comparable DN activity compared to the untagged form (Supplemental Figure 1).

462

463 CARD11 also affects TCR-induced mTORC1 activation (30, 31). We therefore further
464 tested whether selected *CARD11* variants could disrupt TCR-induced mTORC1
465 activation by measuring ribosomal S6 protein phosphorylation by immunoblotting. For
466 most mutations within the CARD domain, we observed a trend toward decreased
467 phospho-S6 (Figure 1C-D), similar to previously characterized DN mutants (9). These
468 differences did not reach statistical significance, however, due to inherent variation in
469 our assays. mTORC1 signaling is exquisitely sensitive to subtle perturbations in cell
470 viability, culture media contents and stimulation conditions, particularly in Jurkat T cells
471 (K. Hamilton, personal communication). Interestingly, some mutants (e.g. p.R72G,
472 p.R187P) had no appreciable effect on TCR-induced S6 phosphorylation despite
473 impaired NF- κ B activation in Jurkat transfectants (Figure 1C-D). Collectively, these
474 transfection results suggest *bona fide* DN mutations in *CARD11*, often located in the
475 CARD domain, attenuate TCR-induced NF- κ B activation with variable effects on
476 mTORC1 signaling (Figure 1E).

477

478 **Patient phenotypes with dominant negative *CARD11* mutations**

479 We compared a total of 60 patients from 32 kindreds carrying heterozygous *CARD11*
480 variants (Table 1). Including those previously published (7, 9), we identified 28 distinct
481 *CARD11* alleles, of which 14 are DN as determined by the functional assays described
482 above. All kindred pedigrees with confirmed *CARD11* DN variants are shown in Figure
483 2. All patients were referred with immunological phenotypes for investigation, typically
484 presenting in childhood. We therefore compared the manifestations in those with
485 functional *CARD11* DN defects to those with no obvious DN functional defect, even if
486 hypomorphic (Tables 1-2). Severe atopic dermatitis (AD) was present in most patients
487 with DN mutations (32/44; 73%), compared with non-DN variants (5/16, 31%). Other

488 atopic symptoms were noted in patients with DN variants, including asthma (55%) and
489 food allergies (32%), and less frequently, rhinitis and eosinophilic esophagitis (Table 1).
490 Cutaneous viral infections were also more common in patients with DN alleles, including
491 molluscum contagiosum (52%), cutaneous herpes simplex virus type 1 (HSV-1)
492 infection (30%) and warts (27%) (Table 1). We also observed cases of neutropenia,
493 presentations similar to other syndromes associated with elevated IgE and infection
494 (Kindred 14), including IPEX-like syndrome (Kindred 4) in patients with functional DN
495 alleles, but not in the others. Of note, the patient with IPEX-like presentation (including
496 failure to thrive, bloody diarrhea, and severe eczema) carried the identical mutation
497 (p.R30W) to that described recently by Roifman and colleagues (Kindred 5) in a family
498 with severe atopy, infection and mild (late onset) autoimmunity (7). Prominent
499 phenotypes in the collective *CARD11* DN patient cohort are summarized in Table 2. In
500 addition to atopic disease (89%), significant viral skin infections (68%) and lung disease
501 (e.g. infections, pneumonia, bronchiectasis) (68%) were the most prominent symptoms
502 shared by patients harboring DN *CARD11* mutations (Table 2). Additional phenotypes
503 included autoimmunity (20%)—most commonly alopecia, but also including ITP and
504 bullous pemphigoid. Neutropenia was also observed in five patients (14%, including four
505 with no demonstrable atopic disease), although an autoimmune etiology could not be
506 confirmed. Oral ulcers were also observed (14%), and may be linked to neutropenia.
507 Four patients had lymphoproliferative disease (large granular lymphocytic leukemia
508 (LGL), peripheral T-cell lymphoma, and/or mycosis fungoides). Notably, three patients
509 from two families had little to no atopic disease (one had a mild IgE elevation without
510 clinical manifestations), but did have neutropenia with humoral defects including
511 progressive B-cell lymphopenia, poor class switched B-cell memory, and antibody
512 deficiency. Indeed, low IgM and impaired humoral responses to certain vaccines (e.g.
513 pneumococcal) were observed in several patients. Relevant immunological phenotypes,
514 including total and specific antibody defects and lymphocyte subsets are summarized in
515 Table 3 and Online Repository Table 1.

516

517 Hierarchical clustering with a complete linkage algorithm and an asymmetric binary
518 distance measure was used to explore the cohort for specific phenotypic patterns for

519 patients (n=36) and phenotypes (n=7) for which phenotypic data were more complete.
520 While the small size of the cohort precludes any assessment of statistical
521 significance, descriptively we saw (a) a cluster of neutropenic patients having low IgM
522 and lower IgE, (b) patients with AD and asthma who had low IgM, (c) patients with AD
523 without asthma who had low IgG and low IgA, and (d) patients with high IgA, normal
524 IgM, lack of neutropenia and IgE levels that tracked with the presence of AD
525 (Supplemental Figure 2A). These clusters did not appear to correlate with specific
526 mutations. To be more inclusive of phenotypes with some missing data, we performed
527 an additional analysis using all phenotypes (n=31) and patients (n=44). Data was
528 transformed into a Gower distance matrix and reduced to 2-dimensions using t-
529 Distributed Stochastic Neighbor Embedding (tSNE) before applying K-means clustering
530 to partition the patients into three clusters. Supplemental Figure 2B summarizes
531 phenotypes characteristic of each cluster. Interestingly, cluster 2 was characterized by
532 lack of AD, skin bacterial infections, pneumonia, and allergic rhinitis, but included
533 patients with neutropenia and abnormal IgM and IgA levels. This cluster included all
534 patients with R30G and R974C, most patients with R47H, and the single patient with
535 R75Q. Again, all phenotypic correlations predicted by these clusters are merely
536 descriptive for this limited patient cohort.

537

538 The largest family analyzed included ten patients from the United Kingdom (Kindred 14)
539 who presented with autosomal dominant inheritance of symptoms typically associated
540 with DOCK8 deficiency, including elevated serum-IgE levels with significant atopic
541 disease, recurrent respiratory tract infections, skin abscesses, and recurrent or
542 persisting viral skin infections such as molluscum contagiosum, herpes infections or
543 warts (Table 1, Figure 3). Two patients additionally had mycobacterial complications.
544 Surprisingly, mild skeletal/connective tissue abnormalities characteristic for the STAT3-
545 DN autosomal dominant HIES were also observed in six out of ten affected family
546 members. Patient III.4 died from disseminated mycosis fungoides. Immune phenotyping
547 of patient PBMCs from this family revealed low CD8+ T cell numbers and high CD4+ T
548 cell numbers, with a shift towards the naïve compartment and reduction of memory
549 CD4+ T cells. The B cell compartment was normal.

550

551 Flow cytometric analyses of other patients, when available, often showed B-cell defects
552 including low total/memory B cells in those with specific antibody deficiency, and low
553 IgM in several patients (Table 3). Other assays performed showed diminished mitogen-
554 induced T-cell proliferation in the majority of patients tested, and relatively normal
555 frequencies of regulatory T-cells, as previously reported (Table 3). Detailed clinical and
556 laboratory findings for individual patients, where available, are included in Online
557 Repository Table 1.

558

559 **Primary cell signaling defects in CARD11 DN patient lymphocytes**

560 In seven of the patients with confirmed DN mutations, primary cells were available for
561 evaluation of NF- κ B signaling using short Phorbol 12-myristate 13-acetate (PMA)
562 activation. Hallmarks of TCR-induced canonical NF- κ B activation, including p65
563 phosphorylation and I κ B α degradation, were impaired in all samples tested (Figure 4).
564 Impaired upregulation of activation markers at 24 hours and skewed cytokine secretion
565 was also noted in multiple CD4⁺ T cell patient samples, consistent with previous findings
566 (Supplemental Figures 3-4). Of note, NF- κ B activation in lymphocytes from the patient
567 with the V195L substitution—which was LOF but did not show DN activity in our
568 transfection system—was also abnormal. Because haploinsufficiency does not likely
569 lead to direct DN activity (9), the result suggests either that other lesions explain the
570 cellular and clinical phenotype, or that the effects of this mutation on the pathway are
571 not revealed using our transfection system. The variability in pS6 activation in the
572 primary cell assay precludes making a definitive conclusion regarding its utility, though
573 small but reproducible defects were observed in 4 patients tested from Kindreds 6 and
574 19 (Figure 5A-B). Moreover, we noted a more reproducible diminution of pS6 could be
575 observed in CARD11 DN patient samples activated for 24 hours (Figure 5C).

576

577

578 **Discussion**

579
580 In this report, we describe multiple new DN *CARD11* mutations associated with
581 additional immune-deficient and dysregulatory conditions in human patients. Recent
582 reports identified DN *CARD11* mutations in a handful of patients presenting with severe
583 atopic dermatitis and other allergic conditions, with or without additional infections (7, 9).
584 The substantially larger cohort assembled here illuminates a broader phenotypic
585 spectrum of disease tied to *CARD11* DN mutations, including frequent sinopulmonary
586 infections, cutaneous viral infections, neutropenia, hypogammaglobulinemia, and
587 lymphoma (Table 2). Atopic disease was the cardinal feature noted in most patients
588 (89%), frequently presenting in childhood as atopic dermatitis, but also including
589 asthma, allergic rhinitis, food allergies, and even eosinophilic esophagitis (Table 2).
590 However, atopy was mild or absent in a number of patients examined in this report, with
591 no measured differences in TCR-driven signaling responses. There were no obvious
592 clinical similarities between non-atopic *CARD11* DN patients beyond neutropenia
593 (present in four). It is possible that atopic symptoms improved over time for some older
594 adults for whom detailed clinical history was lacking, similar to previously described
595 patients (9). Furthermore, unrelated patients with the same mutation (e.g. R30Q, R72G)
596 and even family members harboring identical mutations (e.g. p.R47H, p.R187P)
597 demonstrated differences in both the variety and severity of disease symptoms. From
598 our characterization of this expanded patient cohort, we conclude that *CARD11* DN
599 mutations exhibit high penetrance and variable expressivity for several phenotypes that
600 can extend beyond atopy. Other genetic variants or polymorphisms could certainly be
601 influencing the heterogeneity and severity of phenotypes observed in certain patients.
602
603 Lack of atopic disease in patients with biallelic *CARD11* null mutations, associated with
604 SCID, is likely due to the relative lack of lymphocyte effector function (32, 33). However,
605 the absence of atopy observed in certain patients described here with *CARD11* DN
606 mutations, all of whom had lived into adulthood without major intervention, is surprising.
607 Interestingly, unsupervised clustering analyses identified a subset of these patients from
608 four kindreds that presented with neutropenia, abnormal Ig levels, and fewer

609 skin/respiratory infections, although the significance of these associations cannot be
610 formally assessed within this limited cohort. We otherwise noted no particular
611 genotype/phenotype correlations, nor were there patterns of other comorbid conditions
612 that suggested substantially different phenotypic manifestations. Phenotypic variation
613 *within* families suggests that other genetic variants, which may not be pathogenic by
614 themselves, or differences in environmental exposures could influence the phenotype.
615 As more *CARD11* variant patients are found, demographic patterns may be possible to
616 establish.

617
618 Non-atopic phenotypes associated with *bona fide* DN mutations shed new light on
619 important biological functions governed by *CARD11* signaling in lymphocytes. For
620 example, insufficient (e.g. low IgM) or misdirected humoral responses appear to be a
621 common outcome of attenuated *CARD11* signaling, with or without elevated IgE. A
622 number of families presented with more severe humoral defects resembling CVID,
623 which may reflect both intrinsic defects in B cell differentiation and/or poor T cell help.
624 Future studies aimed at elucidating specific abnormalities in class switch recombination
625 and plasma cell differentiation in patient B cells would be helpful. The neutropenia noted
626 in several patients was not associated with obvious bone marrow defects, which could
627 suggest an autoimmune etiology; indeed, *CARD11* is primarily expressed in mature
628 lymphocytes. However, given that this is a diagnosis of exclusion, further investigation is
629 warranted.

630
631 Cutaneous viral infections (e.g. molluscum, HSV-1, etc.) were also common to several
632 patients. Impaired CD8+ T cell immunosurveillance could be a factor, and may also help
633 to explain tumor development in certain patients. Interestingly, BENTA patients carrying
634 GOF *CARD11* mutations often present with molluscum and other viral infections (e.g.
635 EBV), and are at greater risk of lymphoma/leukemia development (5). Unlike many
636 *CARD11* DN patients, BENTA patient T cells are only mildly “anergic” and proliferate
637 relatively well in response to robust stimuli, even though IL-2 production is often
638 reduced (6, 34). There is also no evidence of Th2-skewing or atopy in BENTA patients
639 described to date, although this has not been investigated thoroughly. Further studies

640 are needed to elucidate how dysregulated CARD11 variant signaling leads to abnormal
641 CD4+ and CD8+ T cell responses that might predict expressivity of associated
642 phenotypes (e.g. atopy, viral skin infections). Based on our work and the work of others,
643 we suspect alterations in TCR signal strength, metabolic reprogramming, and actin-
644 dependent adhesion and motility could all be contributing factors (13, 35-38).
645
646 Our workup of 48 new patients encompassing 25 novel/rare variants further clarifies
647 whether mutations in specific regions of CARD11 are more or less likely to be
648 pathogenic (Figure 6). Notably, missense mutations in the N-terminal CARD domain
649 (aa1-110) are most likely to disrupt NF- κ B (and less reliably, mTORC1) signaling,
650 probably by compromising interactions with BCL10 (and by association, MALT1). The
651 N-terminal CC domain (aa130-200) is also a hotspot for pathogenic mutations, although
652 it is still difficult to predict which variants in the CC domain will be LOF or DN; GOF
653 mutations have been identified in the CARD, LATCH, and CC domains (28, 39). In
654 contrast, we have not found DN mutations residing between residues ~200-970,
655 encompassing the C-terminal portion of the CC domain, the flexible linker, and the PDZ
656 and SH3 domains. In fact, two mutations within this region (p.P495S, p.R848C)
657 significantly boosted TCR-induced NF- κ B activity in Jurkat cells; however, more work is
658 required to determine if and how this effect contributes to autoimmune manifestations in
659 these patients. Unlike CARD/CC-associated GOF mutations found in BENTA patients,
660 these mutations did not drive constitutive NF- κ B activation in the absence of antigen
661 receptor stimulation. The linker itself (aa449-667) contains an array of redundant
662 repressive and activating elements that govern the complex intramolecular regulation of
663 CARD11 (40, 41), making it unlikely to find single point mutations in the linker that affect
664 CARD11 signaling. Finally, one new (p.R974C) and one previously confirmed DN
665 mutation (p.R975W) were located in the guanylate kinase (GUK) domain), although
666 nearby variants in this region showed no effect on TCR-induced NF- κ B (p.V983M,
667 p.E1028K, p.D1152N). In the end, LOF and/or DN activity was not detected in all rare
668 variants from patients referred for a variety of phenotypes, including severe atopy.
669 These results highlight the utility of our simple cell transfection assay in addition to the
670 workup of primary patient cells whenever possible—indeed, as highlighted by the

671 patient with the p.V195L mutation, the observed NF- κ B signaling defect detected in
672 primary cells cannot always be ascribed to DN activity. Although defects in mTORC1
673 signaling are also important, even small perturbations in cell culture conditions make
674 quantification of differences in S6 phosphorylation extremely challenging for both Jurkat
675 and primary T cells. Therefore, we cannot currently recommend pS6 quantification after
676 short term stimulation as a diagnostic assay for *CARD11* DN mutations. Our
677 comprehensive allelic series suggests that for *CARD11*, protein domain architecture
678 might predict functional consequences of specific mutations. However, this too will
679 require broader, more detailed structure-function analyses of the *CARD11* protein
680 before predictions could be used for clinical diagnoses.

681 For clinicians, this study also provides an improved differential diagnosis for
682 immune deficiency and dysregulation linked to *CARD11* mutations. An algorithm
683 detailing our strategy for identifying and diagnosing these patients is depicted in Figure
684 6. Heterozygous *CARD11* DN mutations may therefore be suspected and sought -
685 either *via* analysis of existing exomes or included in other gene sequencing panels - in
686 patients with histories of atopy (especially atopic dermatitis), often in combination with
687 sinopulmonary bacterial infections or cutaneous viral infections (Figure 6), especially
688 when a dominant family history of any of those phenotypes is present. Failure to thrive,
689 neutropenia, autoimmunity (e.g. alopecia), specific antibody deficiency and/or CVID,
690 and even lymphoma may also be noted. Even in patients without atopy, but with a
691 family history of dominant inheritance of any of the other phenotypes above, it may be
692 worth testing for a heterozygous *CARD11* DN mutation. A simple lab diagnostic test
693 aimed at uncovering a TCR-induced NF- κ B signaling defect in primary T cells is
694 strongly recommended, even before sequencing is performed. Although identification of
695 such mutations may not alter patient care currently, continued evaluation and reporting
696 of new *CARD11* variants (perhaps through a registry) will advance our understanding of
697 specific phenotypic associations and hopefully inform future clinical management.
698 Certainly, those with any such phenotypes in whom a rare heterozygous *CARD11*
699 mutation is found even by chance should lead to strong suspicion that it is causal,
700 especially if it resides in the CARD domain. Nevertheless, functional tests such as those
701 described here are imperative for definitive diagnosis.

702 Acknowledgements

703

704 We thank the patients and their families for participating in this research. All patients
705 were enrolled on IRB-approved protocols and provided informed consent. We also
706 thank C. Olsen, C. Lake, K. Voss, R. Chand and H. Pritchett for technical assistance
707 and statistical analysis, and Z. Li in the USUHS Genomics core for primer synthesis and
708 Sanger sequencing support. We thank Dr. Lia Menasce and Dr. Patrick Shenjere,
709 Histopathology Department, Christie Hospital, Manchester, UK for histopathologic data.
710 We thank Drs. James R. Lupski, Richard A. Gibbs, and Zeynep H. Coban Akdemir for
711 providing whole exome sequencing and bioinformatics support in the Baylor-Hopkins
712 Center for Mendelian Genomics (NIH grant UM1HG006542), and T.D Andrews and M.
713 Field for bioinformatics support at John Curtin School of Medical Research. This work
714 was supported in part by the Intramural Research Program of the National Institutes of
715 Health, National Institute of Allergy and Infectious Diseases, National Library of
716 Medicine, and the German BMBF grants 01E01303 and 01ZX1306F, the DZIF (TTU
717 07.801), NIAID extramural award R21AI109187, and the SFB1160 (IMPATH), and
718 National Health and Medical Research Council (Australia) Grants 1113577, 1079648.

719

720

721

722 **References**

- 723
- 724 1. Notarangelo LD, Kim MS, Walter JE, Lee YN. Human RAG mutations:
725 biochemistry and clinical implications. *Nat Rev Immunol.* 2016;16(4):234-46.
- 726 2. Juilland M, Thome M. Role of the CARMA1/BCL10/MALT1 complex in lymphoid
727 malignancies. *Curr Opin Hematol.* 2016;23(4):402-9.
- 728 3. Meininger I, Krappmann D. Lymphocyte signaling and activation by the
729 CARMA1-BCL10-MALT1 signalosome. *Biol Chem.* 2016;397(12):1315-33.
- 730 4. Turvey SE, Durandy A, Fischer A, Fung SY, Geha RS, Gewies A, et al. The
731 CARD11-BCL10-MALT1 (CBM) signalosome complex: Stepping into the limelight of
732 human primary immunodeficiency. *J Allergy Clin Immunol.* 2014;134(2):276-84.
- 733 5. Arjunaraja S, Angelus P, Su HC, Snow AL. Impaired Control of Epstein–Barr
734 Virus Infection in B-Cell Expansion with NF- κ B and T-Cell Anergy Disease. *Frontiers in*
735 *Immunology.* 2018;9(198).
- 736 6. Snow AL, Xiao W, Stinson JR, Lu W, Chaigne-Delalande B, Zheng L, et al.
737 Congenital B cell lymphocytosis explained by novel germline CARD11 mutations. *J Exp*
738 *Med.* 2012;209(12):2247-61.
- 739 7. Dadi H, Jones TA, Merico D, Sharfe N, Ovadia A, Schejter Y, et al. Combined
740 immunodeficiency and atopy caused by a dominant negative mutation in caspase
741 activation and recruitment domain family member 11 (CARD11). *J Allergy Clin Immunol.*
742 2017.
- 743 8. Jun JE, Wilson LE, Vinuesa CG, Lesage S, Blery M, Miosge LA, et al. Identifying
744 the MAGUK protein Carma-1 as a central regulator of humoral immune responses and
745 atopy by genome-wide mouse mutagenesis. *Immunity.* 2003;18(6):751-62.
- 746 9. Ma CA, Stinson JR, Zhang Y, Abbott JK, Weinreich MA, Hauk PJ, et al. Germline
747 hypomorphic CARD11 mutations in severe atopic disease. *Nat Genet.* 2017;49(8):1192-
748 201.
- 749 10. Hara H, Yokosuka T, Hirakawa H, Ishihara C, Yasukawa S, Yamazaki M, et al.
750 Clustering of CARMA1 through SH3-GUK domain interactions is required for its
751 activation of NF-kappaB signalling. *Nat Commun.* 2015;6:5555.
- 752 11. Tanner MJ, Hanel W, Gaffen SL, Lin X. CARMA1 coiled-coil domain is involved
753 in the oligomerization and subcellular localization of CARMA1 and is required for T cell
754 receptor-induced NF-kappaB activation. *J Biol Chem.* 2007;282(23):17141-7.
- 755 12. Meyts I, Bosch B, Bolze A, Boisson B, Itan Y, Belkadi A, et al. Exome and
756 genome sequencing for inborn errors of immunity. *J Allergy Clin Immunol.*
757 2016;138(4):957-69.
- 758 13. Lyons JJ, Milner JD. Primary atopic disorders. *J Exp Med.* 2018;215(4):1009-22.
- 759 14. Adzhubei I, Jordan DM, Sunyaev SR. Predicting functional effect of human
760 missense mutations using PolyPhen-2. *Curr Protoc Hum Genet.* 2013;Chapter 7:Unit7
761 20.
- 762 15. Kircher M, Witten DM, Jain P, O'Roak BJ, Cooper GM, Shendure J. A general
763 framework for estimating the relative pathogenicity of human genetic variants. *Nat*
764 *Genet.* 2014;46(3):310-5.
- 765 16. Kumar P, Henikoff S, Ng PC. Predicting the effects of coding non-synonymous
766 variants on protein function using the SIFT algorithm. *Nat Protoc.* 2009;4(7):1073-81.

- 767 17. Schubert D, Klein MC, Hassdenteufel S, Caballero-Oteyza A, Yang L, Proietti M,
768 et al. Plasma cell deficiency in human subjects with heterozygous mutations in Sec61
769 translocon alpha 1 subunit (SEC61A1). *J Allergy Clin Immunol*. 2018;141(4):1427-38.
- 770 18. Silberstein M, Tzemach A, Dovgolevsky N, Fishelson M, Schuster A, Geiger D.
771 Online system for faster multipoint linkage analysis via parallel execution on thousands
772 of personal computers. *Am J Hum Genet*. 2006;78(6):922-35.
- 773 19. Silberstein M, Weissbrod O, Otten L, Tzemach A, Anisenia A, Shtark O, et al. A
774 system for exact and approximate genetic linkage analysis of SNP data in large
775 pedigrees. *Bioinformatics*. 2013;29(2):197-205.
- 776 20. Gower JC. A general coefficient of similarity and some of its properties.
777 *Biometrics*. 1971:857-71.
- 778 21. Kaufman L, Rousseeuw PJ. Finding groups in data: an introduction to cluster
779 analysis: John Wiley & Sons; 2009.
- 780 22. Maechler M, Rousseeuw P, Struyf A, Hubert M, Hornik K. cluster: Cluster
781 Analysis Basics and Extensions. R package version 2.0. 1. 2015. 2017.
- 782 23. Van Der Maaten L. Accelerating t-SNE using tree-based algorithms. *The Journal*
783 *of Machine Learning Research*. 2014;15(1):3221-45.
- 784 24. Witten IH, Frank E, Hall MA, Pal CJ. *Data Mining: Practical machine learning*
785 *tools and techniques*: Morgan Kaufmann; 2016.
- 786 25. Yu L, Liu H, editors. Feature selection for high-dimensional data: A fast
787 correlation-based filter solution. *Proceedings of the 20th international conference on*
788 *machine learning (ICML-03)*; 2003.
- 789 26. Landwehr N, Hall M, Frank E. Logistic model trees. *Machine learning*. 2005;59(1-
790 2):161-205.
- 791 27. Fuchs S, Rensing-Ehl A, Pannicke U, Lorenz MR, Fisch P, Jeelall Y, et al.
792 Omenn syndrome associated with a functional reversion due to a somatic second-site
793 mutation in CARD11 deficiency. *Blood*. 2015;126(14):1658-69.
- 794 28. Chan W, Schaffer TB, Pomerantz JL. A quantitative signaling screen identifies
795 CARD11 mutations in the CARD and LATCH domains that induce Bcl10 ubiquitination
796 and human lymphoma cell survival. *Mol Cell Biol*. 2013;33(2):429-43.
- 797 29. Thome M, Charton JE, Pelzer C, Hailfinger S. Antigen receptor signaling to NF-
798 kappaB via CARMA1, BCL10, and MALT1. *Cold Spring Harb Perspect Biol*.
799 2010;2(9):a003004.
- 800 30. Hamilton KS, Phong B, Corey C, Cheng J, Gorentla B, Zhong X, et al. T cell
801 receptor-dependent activation of mTOR signaling in T cells is mediated by Carma1 and
802 MALT1, but not Bcl10. *Sci Signal*. 2014;7(329):ra55.
- 803 31. Shi JH, Sun SC. TCR signaling to NF-kappaB and mTORC1: Expanding roles of
804 the CARMA1 complex. *Mol Immunol*. 2015;68(2 Pt C):546-57.
- 805 32. Greil J, Rausch T, Giese T, Bandapalli OR, Daniel V, Bekeredjian-Ding I, et al.
806 Whole-exome sequencing links caspase recruitment domain 11 (CARD11) inactivation
807 to severe combined immunodeficiency. *J Allergy Clin Immunol*. 2013;131(5):1376-83
808 e3.
- 809 33. Stepensky P, Keller B, Buchta M, Kienzler AK, Elpeleg O, Somech R, et al.
810 Deficiency of caspase recruitment domain family, member 11 (CARD11), causes
811 profound combined immunodeficiency in human subjects. *J Allergy Clin Immunol*.
812 2013;131(2):477-85 e1.

- 813 34. Brohl AS, Stinson JR, Su HC, Badgett T, Jennings CD, Sukumar G, et al.
814 Germline CARD11 Mutation in a Patient with Severe Congenital B Cell Lymphocytosis.
815 J Clin Immunol. 2015;35(1):32-46.
- 816 35. Aronica MA, Mora AL, Mitchell DB, Finn PW, Johnson JE, Sheller JR, et al.
817 Preferential role for NF-kappa B/Rel signaling in the type 1 but not type 2 T cell-
818 dependent immune response in vivo. J Immunol. 1999;163(9):5116-24.
- 819 36. Pollizzi KN, Powell JD. Integrating canonical and metabolic signalling
820 programmes in the regulation of T cell responses. Nat Rev Immunol. 2014;14(7):435-
821 46.
- 822 37. Rebeaud F, Hailfinger S, Posevitz-Fejfar A, Tapernoux M, Moser R, Rueda D, et
823 al. The proteolytic activity of the paracaspase MALT1 is key in T cell activation. Nat
824 Immunol. 2008;9(3):272-81.
- 825 38. Rueda D, Gaide O, Ho L, Lewkowicz E, Niedergang F, Hailfinger S, et al. Bcl10
826 controls TCR- and FcgammaR-induced actin polymerization. J Immunol.
827 2007;178(7):4373-84.
- 828 39. Lenz G, Davis RE, Ngo VN, Lam L, George TC, Wright GW, et al. Oncogenic
829 CARD11 mutations in human diffuse large B cell lymphoma. Science.
830 2008;319(5870):1676-9.
- 831 40. Jattani RP, Tritapoe JM, Pomerantz JL. Cooperative Control of Caspase
832 Recruitment Domain-containing Protein 11 (CARD11) Signaling by an Unusual Array of
833 Redundant Repressive Elements. J Biol Chem. 2016;291(16):8324-36.
- 834 41. Jattani RP, Tritapoe JM, Pomerantz JL. Intramolecular Interactions and
835 Regulation of Cofactor Binding by the Four Repressive Elements in the Caspase
836 Recruitment Domain-containing Protein 11 (CARD11) Inhibitory Domain. J Biol Chem.
837 2016;291(16):8338-48.
838
839

840 **Figure Legends**

841

842 **Figure 1. Jurkat T cell transfection screens for LOF/DN activity of new CARD11**
 843 **variants. (A)** Quantification of NF- κ B-induced GFP reporter activity in CARD11-
 844 deficient JPM50.6 T cells transfected with empty vector (EV), wild-type (WT), or mutant
 845 CARD11 constructs and subsequently stimulated with anti-CD3/CD28 Abs. Data are
 846 mean \pm SEM for ≥ 3 separate transfections each. **(B)** Quantification of NF- κ B-induced
 847 GFP in JPM50.6 cells transfected with equal ratios of WT and mutant CARD11
 848 constructs. Data are mean \pm SEM for ≥ 3 separate transfections of each LOF variant;
 849 dashed boxes in (A-B) indicate SEM for numerous WT transfections. Asterisks denote
 850 statistically significant reductions in GFP MFI versus WT (A) or WT+WT CARD11 (B)
 851 after stimulation, indicating DN activity ($p < 0.05$). **(C)** Immunoblot for phospho-S6, total
 852 S6, and FLAG-CARD11 expression in Jurkat T cells transfected with CARD11
 853 constructs \pm 20 min stimulation with anti-CD3/CD28 Abs. Data are representative of
 854 several independent experiments. **(D)** Spot densitometric quantification of phospho-
 855 S6/S6 ratio for each mutant, normalized to WT (dashed line = 1). Data are mean \pm SD
 856 for 2-3 experiments for each variant. **(E)** Schematic diagram of CARD11 protein
 857 including new DN, LOF, hypermorphic and benign (i.e. no effect) variants. Stars indicate
 858 mutations with reduced ph-S6 in (D).

859

860 **Figure 2. Pedigrees for new CARD11 DN variants.** Key indicates healthy (white),
 861 affected (symptomatic with confirmed heterozygous DN mutation), and possibly affected
 862 (symptomatic, no genotype available). Asterisks denote patients that were definitively
 863 genotyped.

864

865 **Figure 3. Clinical presentation of patients with DN CARD11 mutations (A) R30Q**
 866 **(Kindred 2) and (B-F) R187P (Kindred 14). (A)** Patient II.1 displaying HSV-1 skin
 867 disease. **(B)** Patient IV.6 displaying severe eczema. **(C)** Cutaneous vasculitis (both) and
 868 alopecia (left) in patient IV.3. **(D)** Chest radiograph of patient III.5 from 2008 depicting
 869 bronchiectasis. **(E)** Abnormal dentition (left) and brachial hypermelanosis (right) in
 870 patient IV.8. **(F)** Histology findings in patient III.4 with cutaneous T cell lymphoma

871 (mycosis fungoides). Left: viable pleomorphic blasts x40; middle: necrotic lymph node
872 replaced by lymphoma low power; right: CD2 staining viable and semiviable cells.

873

874 **Figure 4. Defective NF- κ B activation in primary T cells from CARD11 DN/LOF**

875 **patients. (A)** Primary CD4⁺ and CD8⁺ T cells from 3 Kindred 14 patients (III.1, III.2,
876 IV.4) and 2 controls were left unstimulated (gray filled histograms) or stimulated for 15
877 min with PMA + ionomycin (black histograms). I κ B degradation and p65
878 phosphorylation was detected by intracellular flow cytometry. **(B)** Total PBMC from
879 affected patients, unaffected family members and controls (labeled at right, + standing
880 for WT) were stimulated for 20 min with PMA or left unstimulated (basal: gray
881 histograms). I κ B degradation and p65 phosphorylation was detected in gated CD4⁺ T
882 cells by intracellular flow cytometry. Geometric mean fluorescence intensity (gMFI)
883 values are listed within each histogram.

884

885 **Figure 5. Defective S6 phosphorylation in primary T cells from affected CARD11**
886 **DN patients after acute and prolonged stimulation. (A)** Primary CD4⁺ T cells from

887 affected patients in Kindreds 6, 19 and 29, healthy relatives and controls were not
888 stimulated (NS) or stimulated with PMA for 20 min. S6 phosphorylation was measured
889 by intracellular flow cytometry. **(B)** The ratio of pS6 gMFI for stimulated versus
890 unstimulated cells is plotted for each of 3 experiments represented in (A). Asterisks
891 denote statistical significance relative to controls (Kruskal-Wallis test, $p < 0.05$). **(C)** Total
892 PBMC from affected CARD11 DN patients, controls (C) and travel controls (TC) were
893 cultured under Th0 conditions for 24 hours. S6 phosphorylation was measured in
894 CD4⁺CD45RA⁻ or RA⁺ cells gated for high vs. low side scatter (SSC) by intracellular
895 flow cytometry; % pS6⁺ cells are labeled within each histogram.

896

897 **Figure 6. Clinical diagnostic algorithm for recognizing CARD11 DN patients.**

898 Schematic diagram of an algorithm to be used in identifying and diagnosing potential
899 *CARD11* DN patients. Suspected patients typically present with atopy with or without
900 cutaneous viral infections and respiratory infections. Simple lab diagnostic tests to
901 pinpoint TCR-induced NF- κ B activation defects in primary patient T cells (e.g. phospho-

902 p65, I κ B degradation) are recommended prior to genomic sequencing analysis, or after
903 a *CARD11* mutation is uncovered (e.g. via WES). Within these selected patients, a
904 mutation in the CARD domain (or N-terminal CC domain) is highly likely to be DN,
905 whereas mutations in the rest of the protein are more likely benign. Functional testing
906 (e.g. Jurkat transfection assays for NF- κ B activation) is recommended for all novel
907 *CARD11* variants, especially for those outside the CARD domain.

908

909 **Table 1. Clinical phenotypes for all patients with *CARD11* variants.** Kindreds are
910 listed in the order each variant appears within the *CARD11* protein.

911

912 **Table 2. Clinical summary of *CARD11* DN patients.** Summary table of mean age,
913 gender ratio, and relevant phenotypes shared by *CARD11* DN patients, with the % of
914 affected patients shown for each category.

915

916 **Table 3. Immunological phenotypes for patients with *CARD11* DN variants.**

917 Descriptors are based on institution-specific reference ranges for each parameter (see
918 Online Repository Table 1). Absent = no cells detected, Low = >10% below reference
919 range minimum, Borderline low = within 10% of reference minimum, High = >10%
920 above reference range maximum. Numbers in parentheses = number of patients with
921 the observed defect / number of patients tested within each kindred.

922

Kindred	Mutation	Genotype	Functional defect	# patients	Atopic dermatitis	Asthma	Food allergy	Pneumonia	Bronchiectasis	Molluscum contagiosum	Cutaneous HSV	Warts	Other Phenotypes
1	R30G	c.88C>G	DN	6	1	3	0	1	0	2	0	0	bacterial sinusitis/meningitis, visceral leishmaniasis, severe vernal keratoconjunctivitis, florid EoE, severe oral ulcers
2	R30Q	c.89G>A	DN	1	0	0	1	0	0	0	1	0	bullous pemphigoid
3	R30Q	c.89G>A	DN	2	2	1	2	2	0	2	0	2	viral pneumonia, S. aureus skin infection, flu, constipation
4	R30W	c.88C>T	DN	1	1	0	0	0	0	0	0	0	IPEX-like, FTT
5	R30W	c.88C>T	DN	4	3	4	4	3	1	0	0	0	recurrent respiratory infections, oral candidiasis, lichen sclerosis of vulva, psoriasis, impetigo
6	R47H	c.140G>A	DN	3	1	1	0	0	0	3	3	3	neutropenia, LGL
7	R47H	c.140G>A	DN	1	1	1	0	1	0	1	0	1	progressive hypogammaglobulinemia
8	E57D	c.171A>C	DN	2	2	2	1	2	0	1	0	0	ulcerative colitis, stroke, peripheral T lymphoma
9	R72G	c.214C>G	DN	2	2	2	0	1	1	0	0	1	alopecia, joint pain, oral ulcers, pulm TB
10	R72G	c.214C>G	DN	1	1	1	0	1	0	1	0	0	persistent skin infections (VZV, HPV), EBV viremia, progressive B cell lymphopenia, frequent OM
11	R75Q	c.224G>A	DN	1	0	0	0	0	0	1	0	0	neutropenia
12	L92W	c.275T>G	DN	1	1	0	0	0	0	0	1	0	
13	K143X	c.427A>T	Weak DN	1	1	0	0	0	0	0	0	0	ITP, alopecia, EoE
14	R187P	c.560G>C	DN	10	10	5	4	4	2	8	6	5	alopecia, cutaneous vasculitis, mycosis fungoides, broad nose, retained teeth, shingles
15	dup183-196	c.701_713ins T	DN	3	3	1	0	3	1	2	1	0	prom forehead, broad nose, poor dentition, pulm TB, eosinophilic coloproctitis
16	L194P	c.581T>C	DN	1	1	1	1	0	0	1	0	0	
17	V195L	c.583G>C	LOF	1	1	1	0	0	0	0	0	0	diverticulitis, T2D
18	K362E	c.1084A>G	LOF	1	0	0	0	0	0	0	0	0	healthy
19	R408H	c.1223G>A	LOF	1	0	0	0	1	0	0	0	0	Evan's syndrome, anhidrosis
20	P495S	c.C>T	Hypermorphic w/ TCR stim	1	0	0	0	1	0	0	0	0	IPEX-like, FTT, T1D, alopecia, skin tags
21	I544L	c.1630A>C	Nil	1	1	0	0	0	0	0	0	0	atopic dermatitis
22	R608H	c.1823G>A	Nil	1	1	0	0	0	0	0	0	0	CMV myocarditis, adenoviral hepatitis
23	V659M	c.1975G>A	Nil	1	0	0	0	1	0	0	0	0	recurrent sinopulmonary/skin infections
24	T670M	c.2009C>T	Nil	1	0	0	0	0	0	0	0	0	Seizures, mental retardation, TB, candidiasis, facial dysmorphism
25	E766D	c.2298G>T	Nil	1	1	0	0	0	0	0	0	0	severe atopic dermatitis
26	R848C	c.2542C>T	Hypermorphic w/ TCR stim	2	1	1	0	1	0	0	0	0	AHA, ITP, refractory cytopenias, drug-induced lupus, Crohn's disease
27	R912Q/D1152N	c.2735G>A, c.3454G>A	Nil	1	0	0	0	1	0	0	0	0	late onset recurrent sinopulmonary infections
28	S923L	c.2768C>T	LOF	1	0	0	0	1	0	0	0	0	agammaglobulinemia, giardiasis
29	R974C	c.2920C>T	Weak DN	2	0	1	0	1	0	1	0	0	neutropenia, mycobacterial disease
30	R975W	c.2923C>T	DN	2	2	1	1	0	0	0	1	0	
31	V983M	c.2947G>A	Nil	2	1	1	1	1	0	0	1	0	
32	E1028K	c.3082G>A	Nil	1	0	0	0	0	0	0	0	0	sJIA, MAS, pheochromocytoma, migraines
		DN		13	44	32	24	14	19	5	23	13	12
		%				73%	55%	32%	43%	11%	52%	30%	27%
		Non-DN		15	16	6	3	1	7	0	0	1	0
		%				38%	19%	6%	44%	0%	0%	6%	0%
		TOTAL		28	60	38	27	15	26	5	23	14	12

Table 1. Clinical phenotypes for all patients with *CARD11* variants.

CARD11 DN Patients	
Age (mean \pm SD)	23.3 \pm 19.5
Age of disease onset (mean \pm SD)	5.2 \pm 6.7
% Female	50%

Clinical Phenotype	% Patients Affected
Atopic disease	89%
Atopic dermatitis	73%
Asthma	55%
Food allergies	32%
Eosinophilic esophagitis	7%
Cutaneous viral infections	68%
Respiratory infections	68%
Autoimmunity	20%
Neutropenia	14%
Oral ulcers	14%
Hypogammaglobulinemia	11%
Lymphoma	7%

Table 2. Clinical summary of *CARD11* DN patients.

Kindred	Mutation	# patients	T cell prolif defect	Spec Ab response defect	Total Ab defect	Total CD4	Memory CD4	Total CD8	Memory CD8	Total B cells	Low CS/Mem B cells	NK cells	Tregs	IgE	Eosinophils
1	R30G	6	no	yes (2/6)	no	normal	ND	normal	ND	normal	normal	normal	ND	high (3/6)	high (2/6)
2	R30Q	1	yes	yes	yes (low IgM)	normal	normal	normal	normal	borderline low	ND	borderline low	ND	high	high
3	R30Q	2	yes (2/2)	yes (2/2)	yes (2/2)	normal	normal	normal	normal	normal	low	normal	ND	high (2/2)	high (1/2)
4	R30W	1	unknown	unknown	unknown	unknown	unknown	unknown	unknown	unknown	unknown	unknown	low	high	ND
5	R30W	4	yes (4/4)	yes (2/4)	yes (2/4)	normal	ND	normal	ND	low (1/4)	ND	normal	ND	high	high (3/4)
6	R47H	3	yes (3/3)	yes (2/2)	yes (1/3)	normal	low (3/3)	normal	low (3/3)	normal	low (3/3)	normal	normal	high 1/3	normal
7	R47H	1	yes	yes	yes	normal	low	normal	ND	low	low	normal	normal	high	normal
8	E57D	2	yes (1/2)	unknown	yes (1/1)	normal	ND	normal	ND	normal	normal	low (1/2)	normal	high	high
9	R72G	2	yes (1/2)	yes (2/2)	no	normal	ND	normal	ND	low (1/2)	absent	normal	ND	ND	ND
10	R72G	1	no	yes	no	high	normal	high	normal	low	normal	normal	normal	high	high
11	R75Q	1	yes	yes	no	normal	normal	normal	normal (high TEMRA)	low	low	low	low	normal	normal
12	L92W	1	ND	no	yes	normal	normal	normal	normal	normal	normal	normal	normal	high	ND
13	K143X	1	ND	yes	yes	normal	normal	normal	normal	normal	normal	normal	normal	normal	normal
14	R187P	10	ND	yes (2/10)	yes (1/10)	high (3/3)	low (3/3)	low (1/3)	ND	low (1/3)	low (1/3)	low (3/4)	normal (0/3)	high (8/10)	high (8/10)
15	dup183-196	3	yes (3/3)	no	no	normal	ND	normal	ND	low (1/3)	ND	normal	normal	high	high
16	L194P	1	yes	yes	no	normal	borderline low	normal	borderline low	normal	normal	normal	normal	high	high
29	R974C	2	no	yes (2/2)	IgA (1/2)	normal	normal	normal	normal	normal	normal	normal	normal	normal	normal
30	R975W	2	yes (1/2)	no	no	normal	borderline low (1/2)	normal	normal	normal	normal	borderline low	normal	high	high
	TOTAL	44	61% (19/31)	49% (20/41)	29% (12/42)										

Table 3. Immunological phenotypes for patients with *CARD11* DN variants.

ACCEPTED MANUSCRIPT

ACCEPTED MANUSCRIPT

ACCEPTED MANUSCRIPT

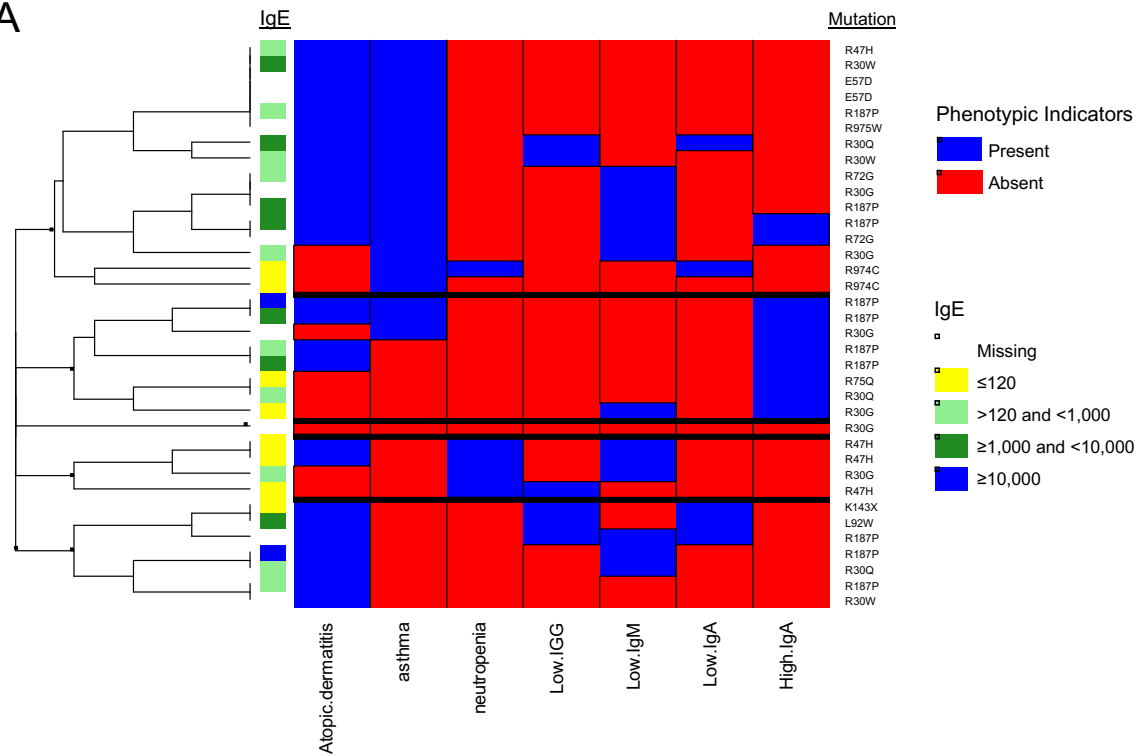
ACCEPTED MANUSCRIPT

ACCEPTED MANUSCRIPT

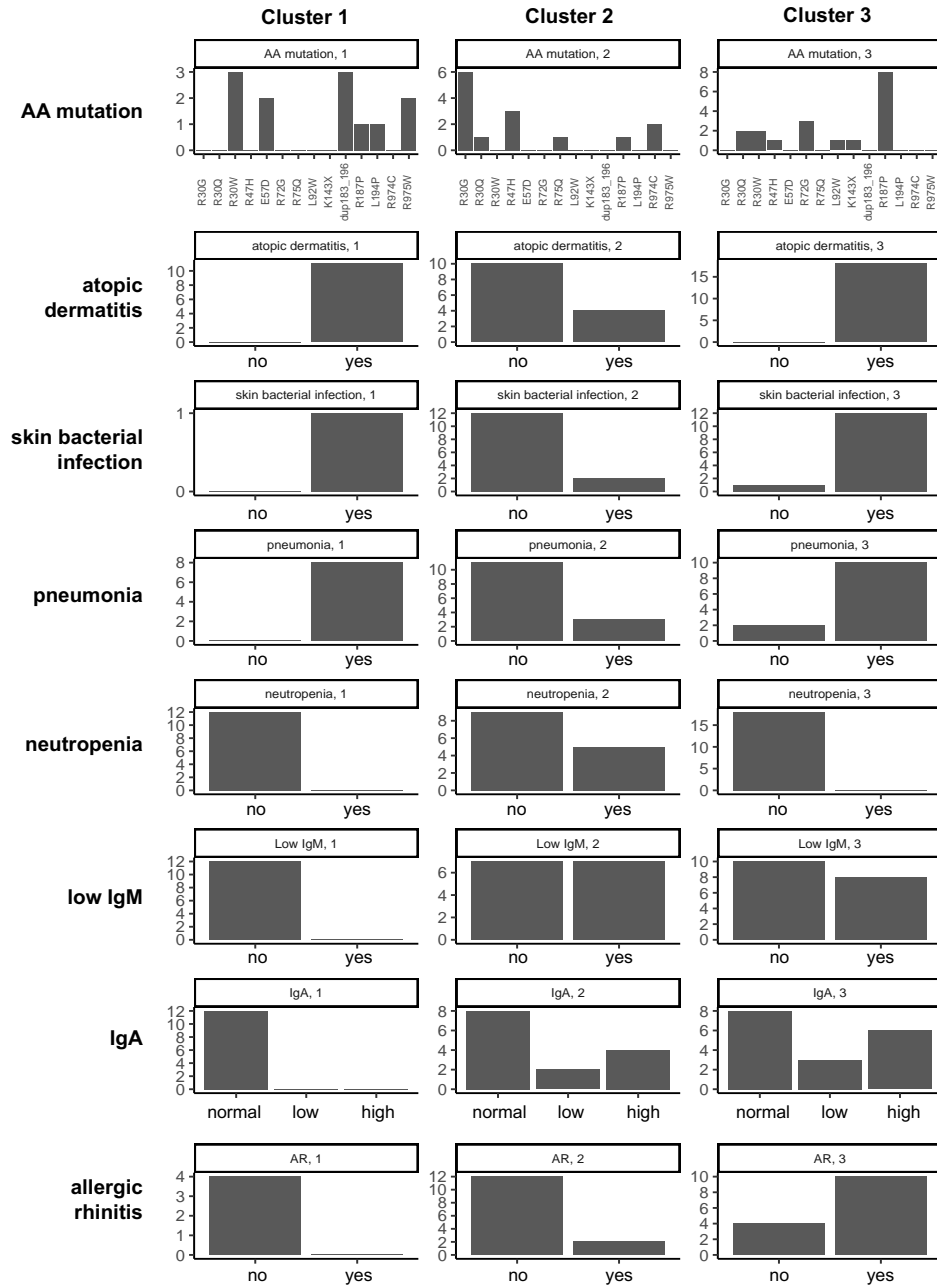
ACCEPTED MANUSCRIPT

ACCEPTED MANUSCRIPT

A



B



ACCEPTED MANUSCRIPT

ACCEPTED MANUSCRIPT

ACCEPTED MANUSCRIPT